Spin-flop bicritical point in MnF_2

A. R. King
Department of Physics, University of California, Santa Barbara, California

H. Rohrer
IBM Zurich Research Laboratory, 8803 Rüschlikon, Switzerland

(Received 19 April 1978; revised manuscript received 28 December 1978)

From measurements of the susceptibility and rf absorption, we have determined the phase diagram of MnF_2 near its bicritical point which is located at $T_B = 64.792 \pm 0.001$ K and $H_B = 118.353 \pm 0.01$ kOe. Alignment of easy axis and applied field was achieved within 2×10^{-6} rad. We find, quite accurately, an anisotropy crossover exponent $\phi = 1.279 \pm 0.031$, in good agreement with renormalization-group predictions for an $n = 3$ component system. However, the less exactly determined amplitude ratio $Q = 1.56 \pm 0.35$ of the two phase boundaries to the paramagnetic state, lies between that predicted for $n = 3$ and that for $n = 2$. The nonuniversal slope q of the $\tilde{t} = 0$ scaling axis is $q = (1.19 \pm 0.15)\times10^{-6}$ (kOe^{-2}) and the amplitude w_+ for the spin-flop to paramagnetic phase boundary is $w_+ = (2.67 \pm 0.3)\times10^{6}$ (kOe^2).

I. INTRODUCTION

Multicritical points and crossover phenomena have received a great deal of attention in the past years.[1] Whereas tricritical points have been extensively investigated in various systems, studies on bicritical and tetracritical points were only recently initiated by the work of Nelson and Fisher, and Kosterlitz, Nelson, and Fisher[2] for magnetic systems, and Aharony and Bruce[3] for structural transitions. One of the interesting aspects of multicritical points is the new critical behavior[1-3] which arises from the competition of different types of ordering and which is dominated by a new set of critical exponents, namely, the anisotropy crossover exponents. In the case of bicritical points, it was shown that the way the two second-order phase-transition lines come into the bicritical point is determined by the second-order anisotropy crossover exponent, ϕ. The experimental determination of these λ lines thus gives direct access to ϕ.[4-14] In the present paper, we report on the experimental determination of the bicritical lines in MnF_2. A short account of this work appeared earlier.[6]

In an easy-axis antiferromagnet, a first-order spin-flop (SF) transition line separates the antiferromagnetic (AF) state from the spin-flop state if the applied field points along the easy axis, as sketched in Fig. 1(a).[4,15] Except for the canting of the sublattices, the spin-flop state can be viewed as an easy-plane (in the uniaxial case) or easy-axis (in the biaxial or orthorhombic case) antiferromagnetic configuration with an effective preferred direction perpendicular to the intrinsic one. The field applied along the easy axis $H_\parallel$, therefore, tunes the effective anisotropy. This effective anisotropy determines the type of order, and thus, the kind of critical fluctuations at the second-order transition lines from the paramagnetic (PM) to the ordered states. At the PM-AF transition line, only the parallel spin components become critical and therefore $n = n_\parallel = 1$, where n is the number of critical spin components (or the dimension of the order-parameter space of the ordered phase). At the PM–spin-flop transition, we have $n = n_\perp = 2$ in the uniaxial case and $n = n_\perp = 1$ in the biaxial one. In the latter case, the critical fluctuations of one of the perpendicular spin components remains uncritical since the effective anisotropy along the hard direction is not affected by $H_\parallel$.

At T_B, H_B the relevant part of the effective anisotropy is zero and the number of critical spin components is $n = n_\parallel + n_\perp$. Thus, $n = 3$ for uniaxial symmetry and $n = 2$ in the biaxial case. An increased number of critical spin components lowers the critical temperature and gives rise to the umbilical nature[15] of the phase diagram at the bicritical point. The phase boundaries in the vicinity of the bicritical point are given by[2,15]

$$\tilde{g} = \pm w_\pm \tilde{t}^{\,\phi}, \tag{1}$$

with the linear scaling fields[16]

$$\tilde{g} = g - pt \tag{2a}$$

and

$$\tilde{t} = t + qg, \tag{2b}$$

where $t = (T - T_B)/T_B$ and $g = H^2 - H_B^2$ with T_B and H_B the temperature and field at the bicritical point; w_+ is the amplitude of the spin-flop–PM boundary,

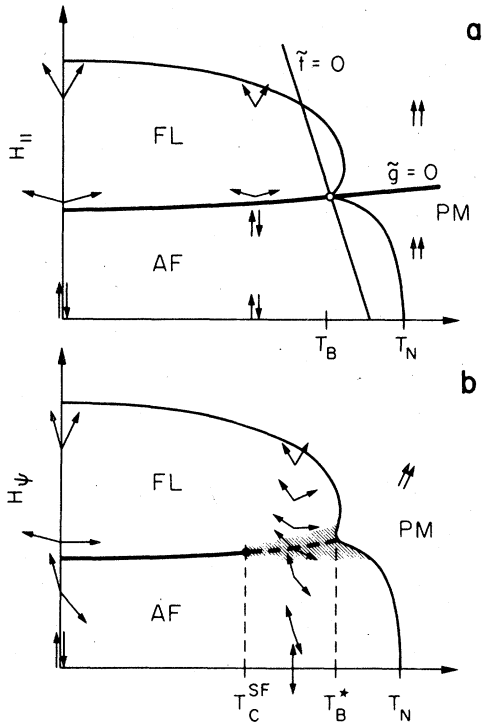

FIG. 1. Schematic phase diagram of uniaxial antiferromagnet (a) for perfect alignment of easy axis and applied field, and (b) easy axis and applied field at angle ψ. (a) also indicates the orientation of the appropriate scaling axis $\tilde{t}=0$ and $\tilde{g}=0$. The shaded part in (b) shows the transitionless region of fast but continuous rotation of the sublattices between the end-point of the SF-transition line T_c^{SF} and the pseudobicritical point $T_B{}^*$.

and w_- is that of the AF-PM boundary. $\tilde{g}=0$ is a natural scaling axis, tangent to the spin-flop transition at the bicritical point[16,17]; analogous to the appropriate scaling axis at critical and tricritical points. The direction of the second scaling axis is, in principle, arbitrary for $\phi>1$, but determines the range over which the leading scaling terms provide a satisfactory description.[15] For maximal range, this axis is not, in general, perpendicular to the temperature scaling axis. Fisher[15,16] derived for the slope q of the field scaling axis

$$q=\frac{n+2}{3nT_B}\left(\frac{dT_c}{d(H^2)}\right)_{H=0}, \tag{3}$$

where $n=3$ for the uniaxial symmetry and $n=2$ for biaxial symmetry, and $T_c(H)$ is the AF-PM transition line. The slopes q and p of the two scaling axes are nonuniversal, likewise the critical-field amplitudes w_+ and w_-. However, the ratio $Q=w_+/w_-$ is, besides the crossover exponent ϕ, a universal constant. The experimental determination of these two universal constants will be of prime interest in the present paper.

MnF_2 is a well studied antiferromagnet with uniaxial anisotropy and is an $n=3$ component system. Theory predicts[2,18] $\phi(n=3)=1.25$, a value only slightly higher than the 1.175 expected for orthorhombic ($n=2$ component system) anisotropy. However, the universal ratio Q of the amplitudes for the two PM-transition lines, differs significantly: $Q(n=3)=2.51$, whereas $Q(n=2)=1.0$.[15,16] Thus, the present investigation serves as a complementary test to the case of orthorhombic $GdAlO_3$ and $NiCl_2\cdot 6H_2O$ reported previously.[4,5]

The gross features of the phase diagram of MnF_2 have been studied by Shapira *et al.*[19] Recently, Shapira and Becerra presented improved results on the phase diagram of MnF_2 near its bicritical point obtained from ultrasonic attenuation measurements.[7] These measurements extend to considerably higher fields than our data and prove quite useful for the fitting of experiment to theoretical predictions. Besides the considerably increased resolution in the present experiment, we have paid careful attention to the problem of aligning the easy axis of magnetization with the applied field. The importance of alignment has been discussed in detail previously.[4,15] At finite misalignment angle ψ, the first-order spin-flop transition line is no longer connected to the PM-transition line but ends in a critical point T_c^{SF}, (Refs. 4, 15, and 20) as shown in Fig. 1(b). In the transitionless region above T_c^{SF}, one still finds a peak in the susceptibility at a field corresponding to the SF-transition field for perfect alignment.[21,22] At this pseudotransition, the sublattices rotate continuously in a narrow field interval from an AF to an SF-like configuration. The width of this pseudotransition increases with misalignment. Consequently, the two λ lines to the PM state are no longer separated by a bicritical point, since the order changes continuously from Ising-like in low fields to x-y-like at high fields. The λ lines are expected to follow Eq. (1) outside this region of mixed order only. Experimentally, they can be observed for $t>10^{-4}$. Full use of this experimental resolution limits the field width of mixed order to $\Delta H<200$ Oe. As is evident later, this requires alignment of easy axis and applied field to at least 1 millidegree. This clearly demonstrates the importance of alignment.

In the recently investigated cubic antiferromagnets[9] $RbMnF_3$ and $KNiF_3$, such orientation problems of the applied field are avoided. In addition, the number of fitting parameters is reduced by one since the AF state is quenched. Under favorable conditions as for $RbMnF_3$, the experimental value of $\phi(n=3)$ is obtained with excellent accuracy.

Various experimental methods like measurements of the susceptibility,[4–6,12] specific heat,[11] magnetostriction,[8] ultrasonic attenuation,[7,9,10] and, most recently, neutron scattering[13,14] have been used to determine the phase boundaries near the spin-flop bi-

critical point. In the present investigation, we measured the parallel, isothermal susceptibility $\tilde{\chi}_{\parallel}$ and used rf absorption and the resonant ^{19}F NMR enhancement[23] as supporting techniques. In the following, only the aspects of the experimental results vital for the location of the phase boundary will be discussed. A detailed account of the dynamic properties close to the various transition lines will be given elsewhere.

II. EXPERIMENT

The parallel isothermal susceptibility $\tilde{\chi}_{\parallel}$ and the rf absorption in the frequency range 14–180 MHz were measured simultaneously. $\tilde{\chi}_{\parallel}$ is the direct susceptibility, the response of the uniform magnetization to a uniform field. Both field sweeps at constant temperature and temperature sweeps at constant fields were used. The NMR measurements were carried out at constant frequencies in the 500-MHz range. The experiments were carried out on a cylindrical single crystal of MnF_2 18-mm long and 3 mm in diameter with the easy axis of magnetization along the cylinder axis. The demagnetizing field at the bicritical point amounts to 15 Oe (bicritical field $H_b = 118.353$ kOe) and was taken as constant in the temperature and field regions investigated. The experimental setup is shown in Fig. 2. The susceptibility was measured with the mutual induction method with modulation fields of 10 Oe and a modulation frequency of 10 Hz. We did not attempt any accurate, absolute measurements of the susceptibility. The susceptibilities shown on the following figures represent roughly the top 1% of the total susceptibilty. For NMR and rf absorptions, we used a bridge-type spectrometer. The rf coil L_{NMR} and the susceptibilty pick-up coil L_x, each 4-mm long, were wound side by side around the center portion of the sample. The moveable brass block MB serves as sample holder and thermal station for sample, coils, and the inner heater IH. Temperatures were measured with an N_2 vapor-pressure bulb N_2 driving a differential pressure transducer. This guaranteed field-independent temperature measurements. For maximum sensitivity, the reference pressure was chosen close to the pressure to be measured. Relative calibration of the overall system to better than 1 mK was achieved with the temperature dependence of the susceptibility and rf absorption at the spin-flop transition; absolute calibration was achieved against a platinum resistance thermometer Pt in zero field. Absolute calibrations were made only with completely quenched frozen-in flux; remanent flux changed calibrations up to 7 mK. The sensitivity of the vapor pressure made a temperature resolution of better than 1 mK possible. The German-silver capillary, CA, connecting the vapor-pressure bulb with the pressure transducer was heated in order to avoid cold spots. Its temperature was controlled by Cu-Constantan thermocouples at various places indicated by stars. The thermocouple nearest to the vapor-pressure bulb served as reference. Thermal contact between vapor-pressure bulb and sample was established by a sapphire rod SA giving a thermal lag between the vapor pressure and sample temperature of a few seconds. Surrounding the sample and vapor-pressure bulb was a copper shield Cu wound nonuniformly with a resistance wire heater IH. Temperature stabilization to better than one part in 10^{-5} was accomplished with a standard temperature controller driving this resistance heater. The temperature of the inner Dewar wall was adjusted by a separate heater AH and residual pressure in the vacuum space, so as to give good temperature control by the inner heater at minimum heating power. Field measurements were made with NMR of a proton sample H_2 in a small coil mounted near the sample. Alignment of the sample within 10^{-4} rad was accomplished by tilting the moveable brass block by means of the two adjusting rods, AR (only one shown in Fig. 2). Fine adjustments were made by tilting the

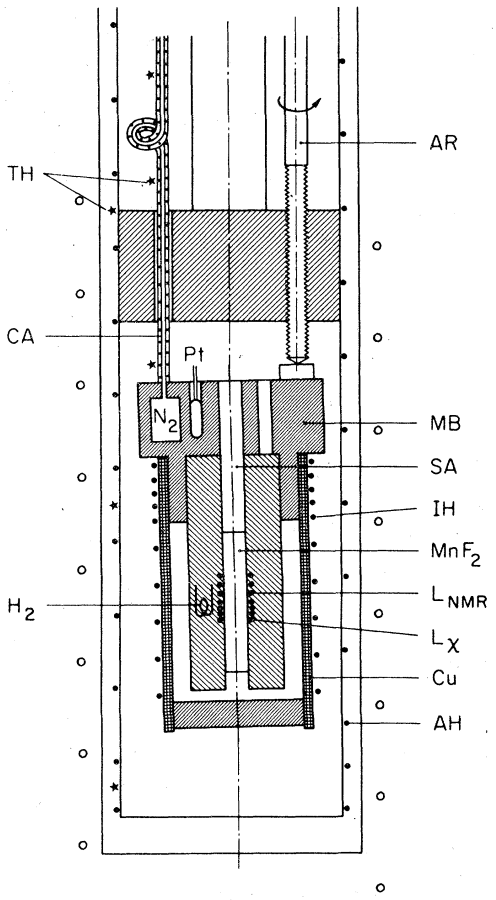

FIG. 2. Schematic of sample holder. The notation is described in the text.

field at the sample with a small field from a pair of Helmholtz coils mounted outside the magnet Dewar, transverse to the large field. The sensitivity of this alignment procedure was about 2×10^{-6} rad. The alignment was checked before each run, and it usually remained unchanged from run to run.

III. EXPERIMENTAL RESULTS

In the study of critical behavior it is desirable to locate the critical point independent of the experimental results to be fitted. In the present experiment, the splitting of the first-order SF transition into two λ lines should, in principle, give an adequate location of the bicritical point, although these λ lines meet there tangentially to the SF transition. Unfortunately, the spin-flop–PM transition is only seen in temperature sweeps and cannot be observed close to the bicritical temperature. But another, unexpected splitting of the susceptibility peak at the SF transition locates T_B within 1 mK or 1.6×10^{-5} in reduced temperature. The SF transition has further been used to accurately align the easy axis and external field. Therefore, we first discuss some aspects of the spin-flop transition before turning to the bicritical behavior of the two paramagnetic-transition lines.

A. Spin-flop transition

The first-order SF transition is easily located by a sharp peak in the field dependence of the parallel isothermal susceptibility $\tilde{\chi}_{\parallel}$ and of the rf absorption $\tilde{\chi}_{\parallel}''$. A peak width of about 100 Oe at half the peak height could be achieved at 9 mK below the bicritical point for the best alignment. The width of the peak decreased to about 70 Oe, 30 mK below T_B, and remained nearly constant at lower temperatures. The peak was asymmetric with a maximum slope on the spin-flop side about half that on the AF side. Near T_B, some asymmetry might be expected due to different critical behavior in the AF and spin-flop states. At low temperatures, this should not be important since the stability limits of the two phases are sufficiently away from the actual transition. The same asymmetry is also observed in $GdAlO_3$.[21]

The temperature dependence of the SF-transition field close to the bicritical point determines the orientation of the temperature scaling axis p [Eq. (2a)]. We obtain $p=1.12\times10^4$ (kOe^2) in good agreement with other experiments.[7,19]

As mentioned earlier, final alignment of the easy axis with applied field had to be performed close to the bicritical temperature where the width of the SF-transition shelf becomes very narrow.[4,21,22] There, both susceptibility and rf absorption are very sensitive to alignment, as shown in Fig. 3 for the susceptibility 9 mK below T_B. The susceptibility peak $\tilde{\chi}_p^{SF}$ decreases rapidly with misalignment, but the field of the susceptibility maximum remains unchanged.[24] Smearing-out of the SF transition occurs mainly towards the AF side. Part of the susceptibility peak is due to critical effects. Their contribution is of the order of the susceptibility peak at the bicritical point, thus only of the order of 10% of the measured SF-transition peak. In addition, no substantial orientation dependence of $\tilde{\chi}_{\parallel}$ at the bicritical point was found experimentally. Therefore, we attribute the variation of the height of the susceptibility peak at the SF transition with orientation to the first-order nature of the SF transition. The width of the SF-transition shelf, which in the molecular field approximation (MFA) is about 3×10^{-4} deg at this temperature,[21] could not be resolved experimentally, but a best alignment can be determined within 10^{-4} deg. This is, of course, an alignment of an average easy axis with an average direction of the applied field, averaged over some angular spread of the direction of the easy axis, and inhomogeneities of the perpendicular field component. Since $\tilde{\chi}_p^{SF}$ drops to about half within 4×10^{-3} deg, we believe that the angular spreads of the easy axis and applied field are also well within this angle. This is an order of magnitude smaller than the angular spread estimated from inho-

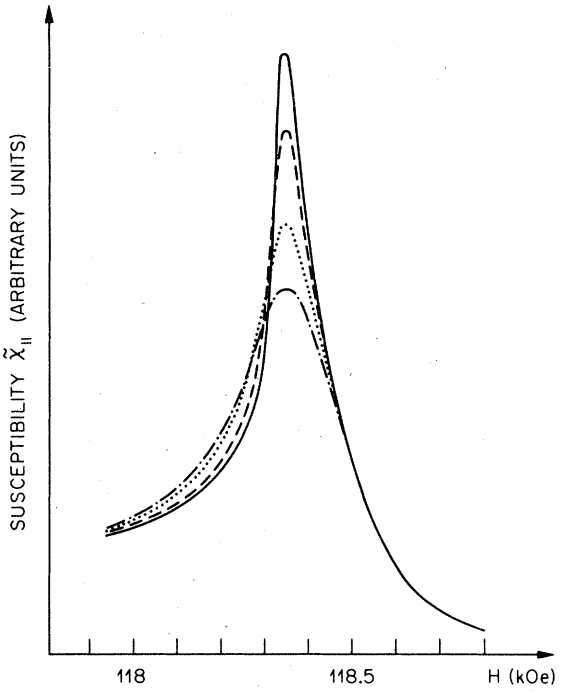

FIG. 3. Susceptibility profile at the SF transition 9 mK below the bicritical point for different alignment angles ψ between easy axis and applied field: best alignment (solid line), $\psi=1.2$ mdeg (dashed line), $\psi=3.6$ mdeg (dotted line), and $\psi=5.4$ mdeg (dash-dotted line).

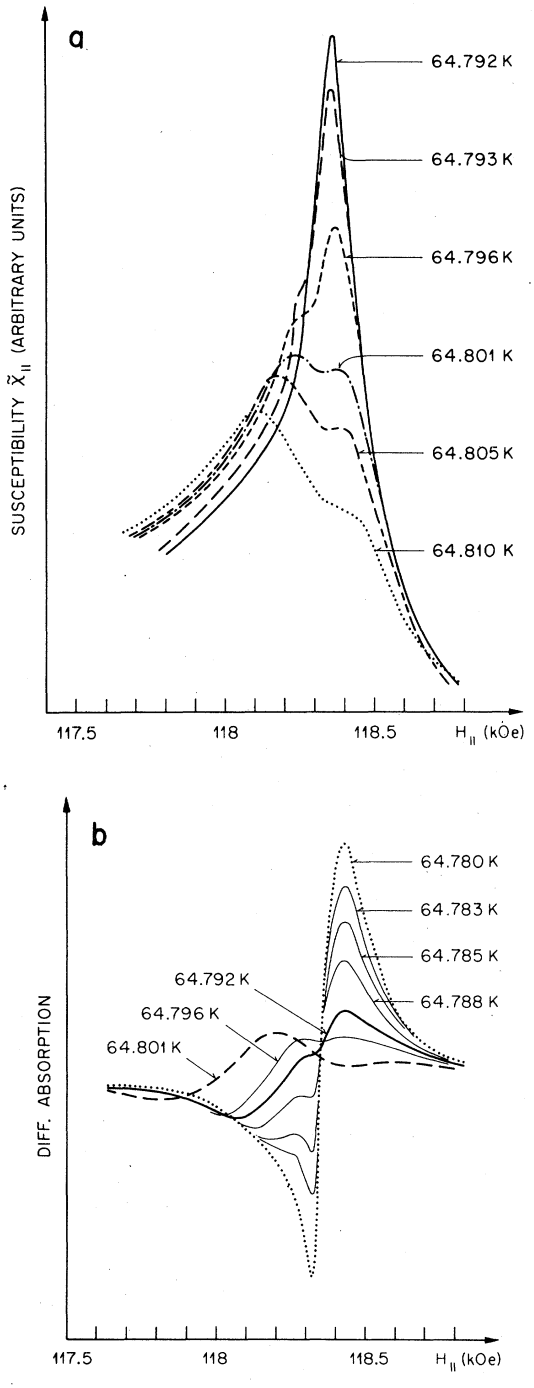

FIG. 4. (a) Susceptibilty profiles in the vicinity of the bicritical temperature for best alignment for different temperatures. The appearance of the shoulder on the low-field side of th susceptibility peak locates the bicritical temperature at 64.792 K. (b) Differential absorption at 14.3 MHz near the bicritical point for different temperatures. At 64.780 K, absorption is observed at the SF transition only; at 64.783 K, an additional absorption in the AF state, cut off by the line at the SF transition, appears.

mogeneous NMR-line broadening.[25] On the other hand, Wong *et al.*[26] derived intrinsic strains in the [110] direction from zero-field circular dichroism, of the order 10^{-5}, compatible with our estimate. The influence of misalignment is almost independent of the azimuthal direction of the misaligned field, as expected for uniaxial symmetry. The small asymmetry observed is attributed to the fact that the principal axis of demagnetization is not perfectly colinear with the easy axis of magnetization.

In the aligned crystal, $\tilde{\chi}_p^{SF}$ and the rf absorption at the SF transition decrease rapidly with increasing temperature. Figure 4 shows the susceptibility and rf-absorption profiles in the vicinity of the bicritical point. The susceptibility peak first decreases linearly with increasing temperature, but before going to zero, a shoulder appears on the low-field side. This shoulder develops into a wide asymmetrical peak. The asymmetrical peak turns out to be the rounded susceptibility divergence at the AF-PM transition. The appearance of the shoulder on the low-field side therefore signals the branching of the AF–PM–transition line and locates the bicritical temperature at 64.792 ±0.001 K. The fitting procedure in Sec. IV confirms that this is the correct bicritical temperature. The intensity of the narrow peak, the remnant of what was the SF-susceptibility

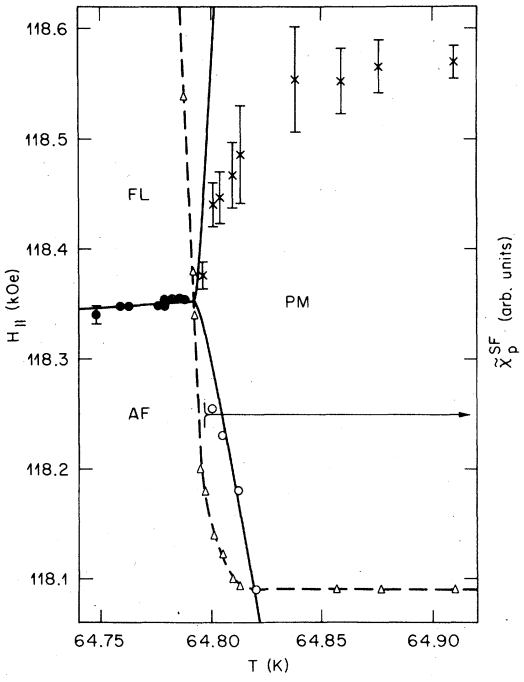

FIG. 5. Location (crosses) and intensity (triangles) of the anomalous susceptibility peak above T_B. Filled circles: SF transition. Also shown are the AF-PM and spin-flop–PM transition lines obtained from a fit to Eq. (1) (solid line) and the experimental points for the AF-PM transition (open circles).

peak, decreases fairly rapidly for some 15 mK above T_B and shifts to slightly higher fields. As is evident from Fig. 5, this anomalous peak is *not* identical with the spin-flop–PM transition.

The origin of this anomalous susceptibility in the PM state is not known at present. A cold end of the sample would see a somewhat smaller field due both to the reduced applied field off-center as well as to larger demagnetization. Its SF transition would, therefore, still be seen above the bulk T_B and at somewhat higher nominal fields. However, the anomaly becomes almost temperature independent at 30 mK above T_B, and exists to at least 150 mK above T_B, the highest temperature at which measurements of this peak have been made. A temperature difference of 150 mK over half the sample length requires heat transport of the order of 100 milliwatts. However, the total power dissipated in the inner and outer heater was as low as 10 milliwatts. In addition, no changes could be observed when varying the total heat dissipated (depending on the vacuum in the dewar wall) or its distribution over the inner and outer heaters. Recent measurements on $GdAlO_3$ also show a similar, double-peak behavior of the susceptibility above T_B in the case of exact alignment of easy axis and applied field, but the anomaly is absent for misalignments of more than some hundredths of a degree.[27] The $GdAlO_3$ samples were small and immersed in liquid helium, therefore field and temperature inhomogeneities as causes of the anomaly can definitely be ruled out. It appears, therefore, that the observed anomaly is not an instrumental artifact. Recent theory,[28] however, does not predict any susceptibility peak at the skewed temperature axis in the PM state. It is not clear, at present, whether this anomaly is an indication of a possibly more complicated phase diagram in the vicinity of a bicritical point.[29]

Consider now the rf absorption. It also exhibits a narrow peak, at the SF transition, whose maximum coincides with the susceptibility maximum within the experimental accuracy. The width of the absorption line is roughly that of the susceptibility peak, but the line is more asymmetric. Domain-wall motion has been suggested as a possible cause of the absorption peak in ultrasound experiments.[19] This does not entirely apply to our case, since the absorption line persists to angles between easy axis and applied field far beyond that where an SF transition can exist. On approaching the bicritical temperature, the absorption line splits into a wide line cut off by the absorption at the SF transition. The absorption pattern is that of a truncated antiferromagnetic-resonance (AFMR) line reported previously for $GdAlO_3$.[30] The truncated AFMR line can be qualitatively understood as follows. The low-frequency AFMR branch is the soft mode in the case of uniaxial symmetry and goes to zero frequency at the stability limit of the AF phase. In spin-flop antiferromagnets, however, the SF transition always occurs experimentally at the thermodynamic transition field (field of equal free energies of the AF and spin-flop states), contrary to the case of metamagnets, where hysteresis at the first-order AF-PM transition is indeed found. The metastable AF region is therefore not accessible experimentally. The width of this metastable region ΔH_{ms} is, in the molecular-field approximation, equal to the width of the SF-transition shelf.[21,24] Therefore, in MnF_2, ΔH_{ms} decreases from about 1 kOe at 0 K to zero at T_B. Sufficiently away from T_B, the AFMR line at our low-measuring frequency lies completely in the unaccessible metastable region. On approaching T_B, the metastable region narrows and part of the AFMR line then appears in the stable AF phase, where it is cut off by the absorption line at the SF transition. Therefore, splitting of the rf-absorption line at the SF transition occurs before the bicritical temperature is reached. Above T_B, the wide absorption line follows the AF-PM transition with nearly a constant field shift. The absorption line at the SF transition, however, does not disappear completely at T_B. As in the case of susceptibility, some anomalous absorption is also found in the PM state above T_B. The center of this weak anomalous absorption line coincides with the peak of the anomalous susceptibility.

The double peak-absorption pattern just below T_B is very sensitive to alignment of easy axis and applied field. Misalignment shifts the AFMR branch to slightly higher frequencies and widens the absorption at H_c^{SF}. A misalignment of 7×10^{-6} rad at 9 mK below T_B, for instance, quenches the truncated AFMR-absorption line completely.

B. AF-PM boundary

The asymptotic behavior of the susceptibility at both the PM-AF and PM–spin-flop transition lines is that of the specific heat[2,31] (except at $H=0$). At the bicritical point, however, χ diverges considerably stronger than the specific heat,[2] i.e., $\tilde{\gamma}=2\phi-\alpha-2$, where $\tilde{\gamma}$ and α are the exponents of the susceptibility and specific heat, respectively. This has been verified experimentally, although the experimental value of $\tilde{\gamma}$ was considerably smaller than predicted.[4] Due to sample, field, and temperature inhomogeneities, a peak in the susceptibility is observed, rather than a divergence. The divergentlike susceptibility peak at the AF-PM transition could be observed equally well in field and temperature sweeps. Field sweeps are more practical experimentally and most of the data for the AF-PM transition were taken by scanning the field at constant temperature. However, the two methods, for the locating of the phase boundary, give identical results. A field scan of both susceptibility

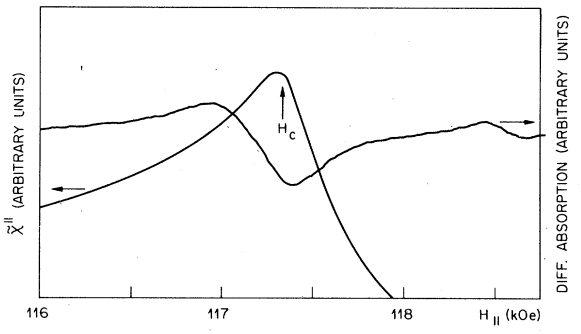

FIG. 6. Differential susceptibility and absorption at the AF-PM transition 79 mK above T_B. The transition field H_c, obtained as described in the text, lies 55 Oe above the field of maximum susceptibility. The maximum of the rf absorption at 14.3 MHz lies clearly below the transition and the absorption extends smoothly through the transition. The center of the anomalous absorption in the PM state at 118.5 kOe coincides with the maximum of the anomalous susceptibility peak.

and rf absorption is shown in Fig. 6, temperature scans of $\tilde{\chi}_{II}$ in Fig. 7. The field or temperature of maximum susceptibility does not coincide with the true or average transition, if the susceptibility peak is asymmetric. The transition is then displaced from the susceptibility maximum towards the steeper side of the peak. Landau and coworkers[32] have analyzed the rounding of the specific heat in $GdCl_3$ and $CoCl_2 \cdot 6H_2O$ in terms of a distribution of local critical temperatures throughout the crystal. They obtained good agreement with experiments assuming a Gaussian distribution. In $GdCl_3$, where the ratio of maximum slopes of the specific-heat peak on the PM side and AF side is about 30, the maximum of the specific heat is shifted downwards by the halfwidth Γ of the distribution. In $CoCl_2 \cdot 6H_2O$, the ratio is only 4, and the shift amounts to about $\frac{1}{2}\Gamma$. Such a detailed analysis of the susceptibility is complicated near the bicritical point by crossover effects. Close to the AF-PM transition line, Ising behavior is expected, crossing over to bicritical behavior further away in the PM state. Indeed, the experimental results well outside the rounded region are not well represented by a single power law. A meaningful distribution width, therefore, could not be derived from the present susceptibility data. Instead, we estimated the displacement of the true $T_c(H_{II})$ from the susceptibility maximum using the specific-heat analysis[32] of $CoCl_2 \cdot 6H_2O$, where a similar ratio of maximal slopes above and below T_c as for $\tilde{\chi}_{II}$ in MnF_2 was found. We note that in the specific-heat case, the distribution is centered at a T_c which lies halfway between the temperature of maximum slope on the PM side and the temperature of the intersection of the maximum slopes on both sides. We applied this to our case assuming that the rounded region of $\tilde{\chi}_{II}$ lies well

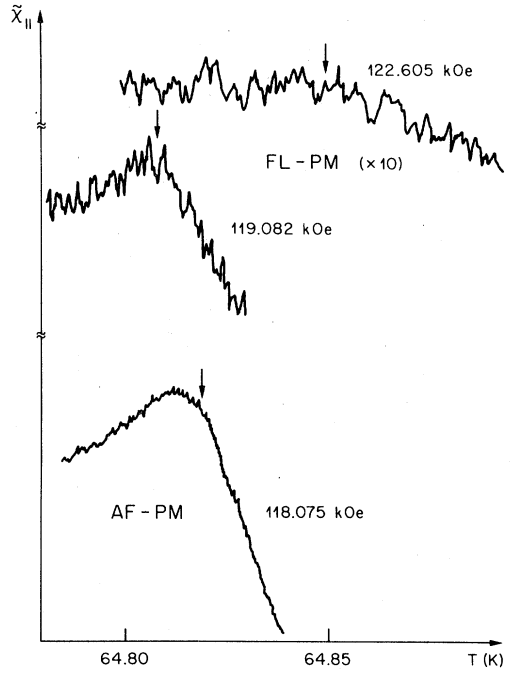

FIG. 7. Differential susceptibility as a function of temperature across the AF-PM boundary ($H = 118.075$) and the spin-flop–PM boundary. The arrows indicate the transition temperature.

within the Ising region. This appears reasonable in view of the narrow rounding region ($\Delta H < 200$ Oe or $t < 6\times10^{-4}$) and the Ising region found for $GdAlO_3$.[4] We then obtained a shift of about 60 Oe at the highest temperatures investigated, corresponding to shifts in critical temperatures from 6 to 10 mK. A rough estimate for the distribution width can be obtained from the width of the SF transition. At sufficiently low temperatures, critical effects are absent and the width of the SF shelf is much wider than the spread in direction of the easy axis. Since the SF-transition field is independent of the angle between easy axis and the applied field,[24] a possible mosaic structure does not broaden the transition. Besides the asymmetric broadening of unknown origin, the main contributions to the width of the T_c distribution $\Gamma(T_c)$, is expected from inhomogeneous isotropic exchange. This gives an upper limit for $\Gamma(T_c)$ of

$$\Gamma(T_c) < \frac{T_c}{4H_{SF}}\Gamma(H_{SF}) ,$$

where $\Gamma(H_{SF})$ is the halfwidth of the SF transition. The factor 4 in the denominator takes care of the square-root dependence of H_{SF} on the isotropic exchange and the contribution of inhomogeneous anistropy to $\Gamma(H_{SF})$. With $\Gamma(H_{SF}) = 70$ Oe, we have $\Gamma(T_c) = 16$ mK. A similar result is obtained if the width of the SF transition is attributed to field gradients. The influence of temperature gradients which

do not affect the SF-transition width is difficult to assess, but is believed to be small. First, no influence of the total heat dissipated and its distribution on the two heaters on the AF-PM transition could be detected. Second, the drastic changes of the susceptibility profiles and absorption patterns near T_B within a few mK also point to temperature inhomogeneities not larger than a few mK. The shifts applied are, therefore, consistent with what one would expect from the different kinds of inhomogeneous broadening.

Associated with the AF-PM transition is an rf absorption. As mentioned above, the absorption pattern just below T_B is typical of a truncated antiferromagnetic resonance (AFMR).[20] As shown in Fig. 4(a), the absorption line associated with the AF-PM transition grows smoothly out of the truncated absorption line. It is therefore implied that the absorption line is due to the low-frequency AFMR. The center of the resonance does not shift with frequency in the frequency range from 118 to 14 MHz, and the absorption amplitude decreases monotonically with increasing frequency. We take this as an indication that the absorption is due to an overdamped mode. Since, at these low frequencies, the line lies very close to the AF-PM transition (within the line width) the rf absorption is dominated by the dynamics of the transition, and is not adequately described by simple AFMR considerations. A detailed discussion of the rf absorption will be given elsewhere.

C. Spin-flop–PM transition

At the spin-flop–PM transition, a susceptibility maximum could only be detected when scanning the temperature at constant field as observed previously in $GdAlO_3$ and $NiCl_2 \cdot 6H_2O$.[4,5] Close to the bicritical point, the maximum of the measured susceptibility was still quite pronounced, but at higher fields only a shoulder in the temperature dependence of $\tilde{\chi}_{\parallel}$ could be seen as shown in Fig. 7. The susceptibility peak, when observed, is very much weaker than at the AF-PM transition. This is expected, since $\tilde{\gamma} = \alpha(n=2) = 0.02$ at the SF-PM boundary compared to $\tilde{\gamma} = \alpha(n=1) = 0.125$ at the AF-PM boundary. On the other hand, a similar effect is also observed in biaxial systems,[4,5] although there $\tilde{\gamma} = \gamma(n=1)$ on both λ lines. In the latter case, it might well be that due to the rather small rhombic anisotropy component, the Ising region at the spin-flop–PM λ line is too narrow to be observed. The ratio of the maximal slopes on the PM and spin-flop sides is about half that at the AF-PM transition. Corrections due to rounding should, therefore, be considerably smaller than at the AF-PM transition. Due to the increased noise of the measured susceptibility, however, application of a similar procedure as in the case of the AF-PM transition is meaningless. Since the maximum or shoulder of $\tilde{\chi}_{\parallel}$ cannot be detemined to better than some 5 mK, (which is larger than the expected correction) the transition was taken to be at the peak or the shoulder of $\tilde{\chi}_{\parallel}$. At some 5 kOe above the bicritical field, the shoulder became too diffuse for accurate location of the phase transition. Better results were obtained there with the method of the resonant NMR enhancement.[23] A detailed account of this resonant NMR enhancement will be given elsewhere. It can be understood qualitatively as follows. The nuclear ^{19}F moments are practically parallel to the applied and rf fields in the spin-flop state. Nuclear transitions are then only induced by the motion of the Mn moments via the hyperfine coupling. The NMR, therefore, probes the perpendicular dynamic sublattice susceptibility $\tilde{\chi}^{\perp}_{\rm sub}(\omega)$. One finds that close to the transition, the NMR enhancement is proportional to $|\tilde{\chi}^{\perp}_{\rm sub}(\omega_{\rm NMR})|^2$, where $\omega_{\rm NMR}$ is the ^{19}F NMR frequency. As long as $\omega_{\rm NMR}$ is slow compared to the eigenfrequency of the Mn moments, $\tilde{\chi}^{\perp}_{\rm sub}(\omega_{\rm NMR})$ can be replaced by $\tilde{\chi}^{\perp}_{\rm sub}(0)$. The latter diverges like $(T_c - T)^{1/2}$ in MFA, thus giving rise to a very large NMR enhancement. However, the eigenmode of the Mn moments excited by a parallel rf field is the soft mode at the spin-flop–PM boundary, and its eigenfrequency will eventually become slow compared with $\omega_{\rm NMR}$ very close to the transition. Then $\tilde{\chi}^{\perp}_{\rm sub}(\omega_{\rm NMR})$ tends to zero and the NMR line disappears at the transition. The lowering of the spin-wave frequency from above $\omega_{\rm NMR}$ to below, when aproaching T_c, is also clearly evident from the observed phase of the NMR signal: the NMR phase was shifted from absorption through dispersion to almost 360 °. The two NMR points in Fig. 7 correspond to vanishing NMR enhancement.

IV. ANALYSIS AND DISCUSSION

The experimental data for the AF-PM and spin-flop–PM boundaries shown in Fig. 8 are now fitted to the form of Eq. (1) by a least-squares fit. For known T_B, this involves four fitting parameters, namely, the crossover exponent ϕ, the amplitude ratio Q, the orientation of the field scaling axis q, and one of the amplitudes, w_+ or w_-. Of main interest, are the two universal parameters ϕ and Q, whereas q and w are nonuniversal. In order to reduce the number of fitting parameters, q has repeatedly been taken from Eq. (3).[5,7] In view of the semiquantitative nature of Eq. (3),[15,16] this appears inappropriate, especially since the choice of q determines, to a great extent, the value of Q.

The experimental uncertainties in locating the transition from the susceptibility peak are considerably larger than errors in field and temperature measurements. The latter are therefore neglected in the following. Since the spin-flop–PM boundary is very

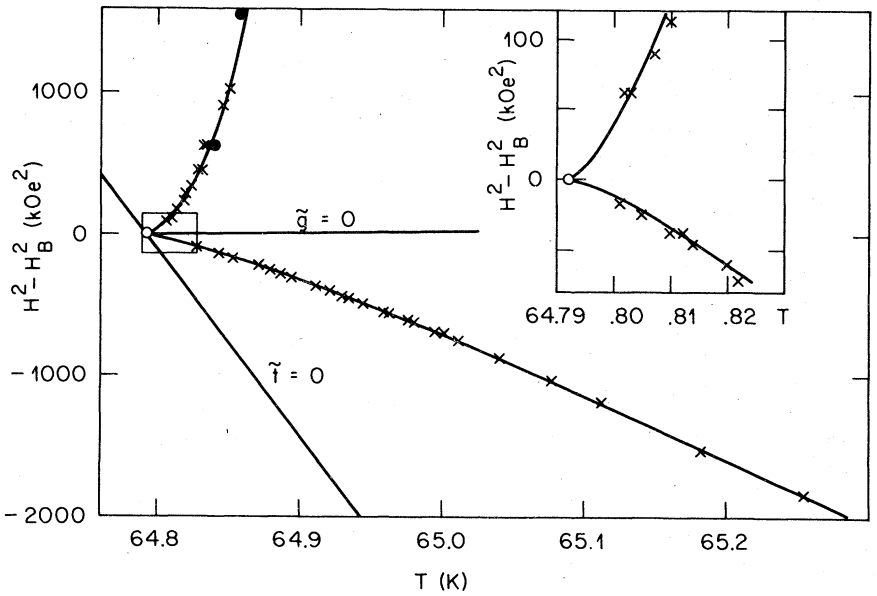

FIG. 8. Phase diagram near the bicritical point. The drawn PM boundary lines and the orientation of the $\tilde{t}=0$ scaling axis correspond to the best fit of the experimental points (crosses) as described in the text. The two filled circles give the spin-flop–PM transition determined from vanishing ^{19}F NMR enhancement.

steep and could only be obtained from temperature-sweep measurements, we took t as the dependent variable with the experimental error. Errors in the location of the critical field in field-sweep measurements are therefore converted into those of critical temperature. The experimental precision is different on the two branches and a weighted least-squares fit is appropriate. At fixed values of ϕ and Q,

$$\chi_\nu^2 = \frac{1}{N-n-1}\sum\left(\frac{\Delta t_i}{\sigma_i}\right)^2 = \sum\left[\left(\frac{\tilde{g}_i}{w_i}\right)^{1/\phi} - qg_i - t_i\right]^2 \tag{4}$$

is minimal for

$$q = \frac{G_H G_T - G_G T_H}{H_H G_G - G_H^2}, \quad w_+ = \frac{G_H}{qH_H + T_H},$$

where

$$G_H = \sum (g_i/\sigma_i^2)|\tilde{g}_i/w_i|^{1/\phi},$$
$$G_G = \sum (g_i/\sigma_i)^2|\tilde{g}_i/w_i|^{2/\phi},$$
$$G_T = \sum (t_i/\sigma_i^2)|\tilde{g}_i/w_i|^{1/\phi},$$
$$H_H = \sum (g_i/\sigma_i)^2, \quad T_H = \sum t_i g_i/\sigma_i^2.$$

t_i,g_i, and $\tilde{g}_i$ are the experimental values of the reduced temperature and field, defined in Eqs. (2a) and (2b). The summations go over all measured points of both branches, with $w_i = w_+$ for the spin-flop–PM branch, and $w_i = w_- = w_+/Q$ for the AF-PM branch.

For each data point, the weighing factor is $1/\sigma_i^2$. For σ_i, we took the estimated precision with which each t_i could be determined, i.e., $\sigma_i = 3\times10^{-5}$ for the AF-PM branch and $\sigma_i = 6\times10^{-5}$ on the spin-flop–PM branch. N is the number of data points, n the number of parameters to be fitted. In our case, $N=67$, $n=4$. A quality criterion of a fit, the χ^2 test, requires $\chi_\nu^2 \lesssim 1$.[33] χ_ν^2 is minimized by

$$\phi = 1.279, \quad Q = 1.56,$$
$$q = 1.19\times10^{-6}(\text{kOe}^{-2}),$$

and

$$w_+ = 2.67\times10^{6}(\text{kOe}^2),$$

with $\chi_\nu^2 = 0.53$. The χ^2 test is, in principle, a valid fitting criterion only if the σ_i's are the experimentally determined standard deviations of representative sets of measurements of t_i at fixed g_i. Since, at most, three data points have been taken at a particular field, we had to use rough estimates for σ_i. The small value of χ_ν^2, therefore, should not be taken as a sign of a particularly good fit, but rather as a consequence of too conservative an estimate of σ_i. Nevertheless, given that these estimates are of the right order, we can consider the fit satisfactory. Since it is not in the spirit of the χ^2 test to adjust σ_i, we continue the analysis with the above estimates of σ_i, but quote in the following the variance of the fit

$$S^2 = N\chi_\nu^2 / \sum_i \sigma_i^{-2}, \tag{5}$$

instead of χ_ν^2. S^2 (or the standard deviation S) depends only on the relative values of the individual sample variances σ_i^2. The standard deviation S should give the reader a better feeling of the quality of the fit; the comparison of S^2 with the weighted average $\bar{\sigma}_i^2$ of the individual variances

$$S^2 \lesssim \bar{\sigma}_i^2 = N / \sum_i \sigma_i^{-2}$$

is equivalent to the χ^2 test. In our case,

$$S = 2.32\times10^{-5}$$

and

$$\bar{\sigma}_i = (\bar{\sigma}_i^2)^{1/2} = 3.5\times10^{-5} .$$

It should be noted that the values of the fitting parameters do not depend strongly on the chosen ratios of σ_i. Setting

$$\sigma_i(\text{AF}-\text{PM}) = \sigma_i(\text{spin-flop}-\text{PM}) = 3\times10^{-5} ,$$

we obtain

$$\phi = 1.292, \quad Q = 1.42 ,$$

$$q = 1.23\times10^{-6}(\text{kOe}^{-2}) ,$$

and

$$w_+ = 2.58\times10^{6}(\text{kOe}^2) ,$$

with $S = 2.45\times10^{-5}$.

The uncertainties of the fitting parameters were obtained by the law of error propagation,[33] e.g.,

$$\sigma_\phi^2 = \sum_i \left(\frac{d\phi}{dt_i}\right)^2 \sigma_i^2 + \left(\frac{d\phi}{dT_c}\right)^2 \sigma_{T_c}^2 + \left(\frac{d\phi}{dH_c}\right)^2 \sigma_{H_c}^2 . \quad (6)$$

The derivatives d/dt_i were obtained numerically, changing t_i by δt_i, one at a time.[10] the change of ϕ (and Q) with T_c is illustrated in Fig. 9(a). We obtain, assuming an uncertainty of 1 mK and 10 Oe in bicritical temperature and field, respectively, and using σ_i (AF-PM) $= 3\times10^{-5}$ and σ_i (spin-flop– PM) $= 6\times10^{-5}$,

$$\phi = 1.279 \pm 0.031,$$

$$q = (1.19 \pm 0.15)\times10^{-6}(\text{kOe}^{-2})$$

$$Q = 1.56 \pm 0.35,$$

$$w_+ = (2.67 \pm 0.3)\times10^{6}(\text{kOe}^2) .$$

The first and second terms on the right-hand side of Eq. (6) are roughly equal, the dominant contribution to the first term being due to the PM–spin-flop branch.

The experimental value of $\phi = 1.279 \pm 0.031$ is in good agreement with the renormalization-group prediction of $\phi(n=3) = 1.25$, and in excellent agreement with the experimental value $\phi = 1.278 \pm 0.02$ found recently in the cubic antiferromagnet $RbMnF_3$.[9] The values of q and Q, however, are considerably smaller than the predicted $q = 1.35\times10^{-6}$ (kOe^2) of Eq. (3) and $Q = 2.51$ of Fisher and Nelson[2] or the $O(\epsilon^3)$ expansion value $Q = 2.33$ of Bruce.[34]

The discrepancy between experiment and theory regarding the nonuniversal parameter q should not be regarded as too serious. Rather, the expression relating q with the slope of the AF-PM boundary at zero field [Eq. (3)] should be considered as a rough estimate.[15,16] In addition, Shapira and Becerra[10] have

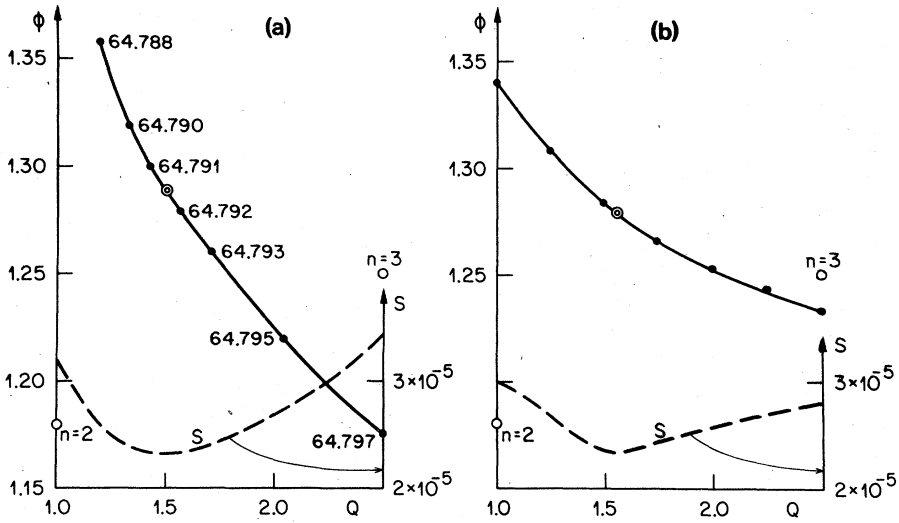

FIG. 9. (a) Best fits for different values of T_c, given by the numbers along the solid line. (b) Best fits for given values of Q with $T_c = 64.792$ K. The two open circles on both figures represent the theoretical values for an $n=2$ and $n=3$ component system. The double circle indicates the absolute best fit on each figure. The dashed lines give the standard deviation of reduced temperature of the various fits.

given some arguments, why Eq. (3) should not be applicable in the case of Cr_2O_3. The same arguments might also be partly responsible for the weaker discrepancy between the experimental q and that derived from Eq. (3) in the case of MnF_2. More serious, however, is the experimentally small value of the amplitude ratio Q. Although the theoretical quotations for Q differ somewhat, Q should definitely be larger than the molecular-field approximation value of $Q=2$.

A first plausible reason for the small experimental value is a possible anistropy in the basal plane, which would make MnF_2 an $n=2$ component system with $Q=1$. Depending on the size of the basal-plane anisotropy, quenching of the perpendicular fluctuations along the hardest axis of anisotropy may be incomplete in the temperature range investigated, and crossover effects should be observed. Fitting the experimental curves to the form of Eq. (1) would then result in effective values of Q between 1 and 2.5, and ϕ between 1.18 and 1.25. There is indeed experimental evidence for a small basal-plane anisotropy as mentioned in Sec. II A. In addition, both low-temperature electronic and ^{55}Mn NMR experiments above the SF transition[35] as well as the resonant NMR enhancement[23] indicate the existence of a low-lying spin-wave mode in the spin-flop phase, and therefore an anisotropy in the basal plane of MnF_2. This anisotropy may be of inhomogeneous origin, as evidenced by the anomalous field dependencies of both the electronic and ^{55}Mn nuclear resonances in the SF state, as well as the nonobservance of the ^{19}F NMR.[35] (A possible fourth-order cubic term should not affect the bicritical properties,[3] i.e., the properties in the $H_{\parallel}-T$ plane.) Another contribution arises from demagnetization. Since the principal axes of demagnetization and the magnetic anisotropy do not exactly coincide, rotational symmetry around the easy axis is not preserved. Whatever the origin of the in-plane anisotropy might be, it is estimated to be of the order of some Oe,[23,25] i.e., three orders of magnitude smaller than the easy-axis anisotropy. Such a small anisotropy should only become effective very close to T_B. Fitting in selected temperature ranges did not give any indication of a crossover from an $n=3$ to an $n=2$ component system. In addition, fits with small Q values give large ϕ and *vice versa,* as shown in Fig. 9(b). We believe, therefore, that the small Q value is not caused by a possible small rhombic component of the anisotropy, because this would imply $Q=1$ and $\phi=1.18$.

A second possible origin for the small Q value might be experimental. We think that the AF-PM boundary is correctly located within 2 mK, but the situation with the spin-flop–PM boundary, especially in the high-field region, is less clear. But it is the spin-flop–PM boundary which dominates the resulting value of Q and a small systematic error in determining the spin-flop–PM boundary from experiment can change Q drastically. A downshift of the experimental spin-flop–PM boundary line by only 10-mK changes the fitting parameters to

$$\phi=1.24,\quad Q=2.4,\quad q=0.89\times10^{-6}(\mathrm{kOe}^{-2})$$

and

$$w_+=2.76\times10^{6}(\mathrm{kOe}^{2})\ ,$$

ϕ and Q thus being close to the theoretical values. Such a fit is, in addition, nearly equivalent in terms of a χ^2 test. However, we think that such a systematical error in the spin-flop–PM boundary is not justified experimentally. Although we have neglected corrections due to rounding at this boundary for reasons given above, such corrections should shift the boundary to higher temperatures. We have also considered the possibility of an incorrect choice of T_c. Figure 9(a) shows the influence of T_c on ϕ and Q. The absolute best fit is obtained with $T_c=64.7915$. This is comforting in respect of our original choice of T_c, but the minimum of χ_ν^2 vs T_c is too shallow in the range of $64.790 < T_c < 64.793$ for an unambiguous choice of T_c on this basis. The important feature is, however, that the curve of best fit comes nowhere close to one of the required values of (ϕ,Q) for $n=2$ or $n=3$.

Our experimental data are further confirmed by the high-field measurements of Shapira and Beccera.[7] Their results are incorporated in Fig. 10 together with the present work. The bicritical points reported are somewhat different from ours. In order to make the best use of their high-field data of the spin-flop–PM boundary not accessible in our experiment, we have adjusted their data for best fit of the AF-PM branch to our data. The relatively large scatter of their data was accounted for by appropriate weighting factors σ_i of 10 mK for the AF-PM branch, and of 20 mK for the spin-flop–PM branch. The fit then gives

$$\phi=1.281\pm0.03,\quad Q=1.54\pm0.3\ ,$$

$$q=(1.21\pm0.2)\times10^{-6}(\mathrm{kOe}^{-2})$$

and

$$w_+=(2.69\pm0.28)\times10^{6}(\mathrm{kOe}^{2})\ .$$

These values agree well with those obtained from the fit to our data above. In particular, the discrepancy of experimental and predicted values for Q remains. We therefore conclude that the low value of Q is neither a consequence of a rhombic anisotropy component nor due to experimental error.

Finally, we should add a word of caution regarding the quality of the fits. From the point of view of the χ^2 test, the quality seems at least reasonable. The resulting standard deviations are in line with the estimated experimental uncertainties. There are, however, two noteworthy features. Firstly, the experi-

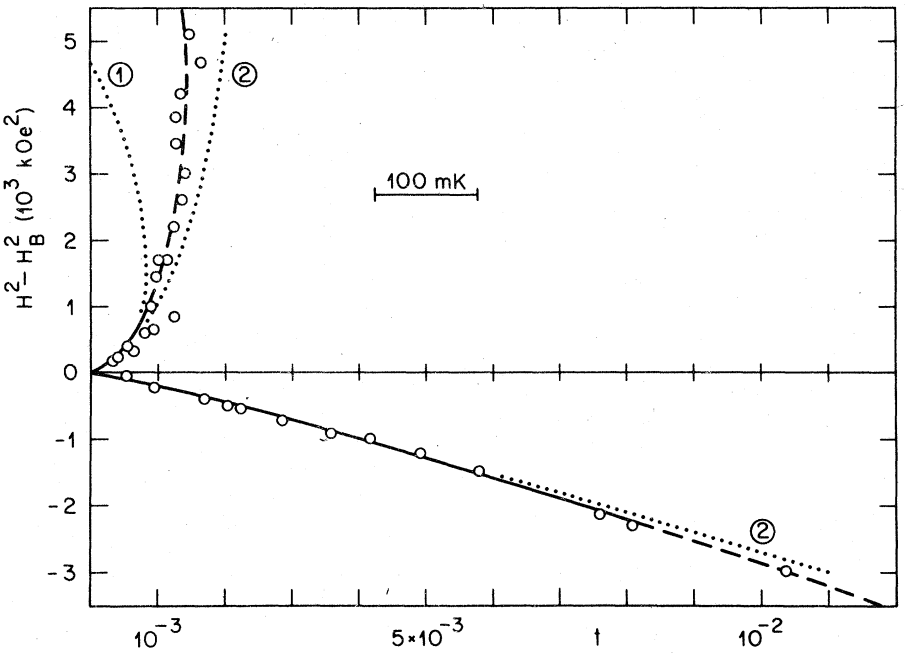

FIG. 10. Comparison of the present data, represented by the solid line, with the high-field data of Ref. 7. The scatter of the present data lies well within the width of the solid line. The heavy solid (range of our data) and dashed line corresponds to the best fit ($\psi = 1.281$ and $Q = 1.54$). The two dotted lines represent fits to our data alone with $Q = 1$, required for an $n = 2$ component system [curve 1: absolute best fit yields $\phi = 1.325$, curve 2: $\phi = \phi(n = 2) = 1.18$].

mental results favor larger values of ϕ (and correspondingly lower values of Q) on the spin-flop–PM branch, and lower values on the AF-PM branch. This was also observed in the case of $GdAlO_3$.[4] Secondly, a small but notable structure of the deviations Δt_i on both branches is found. We take this as an indication of some small systematic discrepancy between the experimental results and the form of the phase boundaries predicted by Eq. (1). Correction terms in Eq. (1) might be necessary for complete agreement with experiment. It might well be that this would also resolve the present problem concerning the experimental value of Q. This conjecture seems supported by Fig. 9(b), which shows ϕ vs Q for fits at fixed T_c. A given value of Q (or ϕ) close to the predicted one, does indeed also imply a value of ϕ (or Q) close to the theoretical one for an $n = 3$ component system but not for $n = 2$. Correction terms in Eq. (1) should not appreciably affect the relation between ϕ and Q in Fig. 9(b), but might well sufficiently shift the rather flat minimum of the resulting standard deviation S to $Q = 2.5$.

V. CONCLUSION

We have determined the phase boundaries near the bicritical point of MnF_2 in the temperature range $10^{-4} < \tilde{t} < 6\times10^{-3}$ for the AF-PM boundary and $10^{-4} < \tilde{t} < 2\times10^{-3}$ for the spin-flop–PM boundary, where $\tilde{t}$ is the reduced temperature with respect to the proper scaling axis. Alignment of easy axis and applied field was achieved within 10^{-4} degrees. The fit of these boundaries to the theoretical expression given in Eq. (1) involves four fitting parameters. We obtain $\phi = 1.279 \pm 0.031$ in good agreement with the predicted $\phi = 1.25$ of an $n = 3$ component system and other experiments in $RbMnF_2$ and Cr_2O_3. There are, however, some problems which are not understood at present.

The most serious one concerns the value of the amplitude ratio Q. We cannot obtain a reasonable fit with the theoretical $Q = 2.5$ for an $n = 3$ component system nor with $Q = 1$ for an $n = 2$ component system. Rather, the experimental evidence supports an intermediate value of $Q = 1.56$. This intermediate value does not reflect a crossover from uniaxial to a possible orthorhombic symmetry. It is conjectured that correction terms in Eq. (1) might well resolve the problem regarding the value of Q.

Secondly, in the paramagnetic state above the bicritical point, an additional, anomalous susceptibility and rf absorption is found. We have no explanation for this "precursor" of the spin-flop transition.

ACKNOWLEDGMENT

Stimulating discussions with Professor A. Aharony, Professor M. E. Fisher and K. A. Müller are acknowledged. One of us (HR) thanks Professor V. Jaccarino from the University of California, Santa Barbara, (where the experiments were performed) for his hospitality and interest in the present work.

[1]A. Aharony, *Proceedings of the International Conference on Magnetism, 1976,* edited by P. F. Châtel and J. J. M. Franse (North-Holland, Amsterdam, 1977), p. 545, and references therein; W. P. Wolf, *ibid.* p. 556.
[2]M. E. Fisher and D. Nelson, Phys. Rev. Lett. 32, 1350 (1974); J. M. Kosterlitz, D. Nelson, and M. E. Fisher, Phys. Rev. B 13, 412 (1976).
[3]A. Aharony and A. D. Bruce, Phys. Rev. Lett. 33, 427 (1974); A. Aharony and A. D. Bruce, Phys. Rev. B 11, 478 (1975).
[4]H. Rohrer, Phys. Rev. Lett. 34, 1638 (1975).
[5]N. F. Oliveira Jr., A. Paduan Filho, and S. R. Salinas, Phys. Lett. A 55, 293 (1975).
[6]A. R. King and H. Rohrer, AIP Conf. Proc. 29, 420 (1976).
[7]Y. Shapira and C. C. Becerra, Phys. Lett. A 57, 483 (1976).
[8]R. D. Yacovitch and Y. Shapira, *Proceedings of the International Conference on Magnetism, 1976,* edited by P. F. Châtel and J. J. M. Franse (North-Holland, Amsterdam, 1977), p. 1123.
[9]Y. Shapira and C. C. Becerra, Phys. Rev. Lett. 38, 358 (1977), Errata. *ibid.* 38, 733 (1977); Y. Shapira and N. F. Oliveira Jr., J. Appl. Phys. 49, 1374 (1978).
[10]Y. Shapira and C. C. Becerra, Phys. Rev. B 16, 4920 (1977).
[11]R. A. Butera and D. R. Rutter, J. Appl. Phys. 49, 1344 (1978).
[12]H. Scharf, H. Weitzel, and O. V. Nielsen (private communication).
[13]J. A. J. Basten (private communication).
[14]J. A. J. Basten, E. Frikkee, and W. J. M. de Jonge, Phys. Rev. Lett. 42, 897 (1979).
[15]M. E. Fisher, AIP Conf. Proc. 24, 273 (1975).
[16]M. E. Fisher, Phys. Rev. Lett. 34, 1635 (1975).
[17]B. Widom, J. Chem. Phys. 43, 3892 (1965); R. B. Griffiths, Phys. Rev. 158, 557 (1967).
[18]D. R. Nelson, J. M. Kosterlitz, and M. E. Fisher, Phys. Rev. Lett. 33, 813 (1974).
[19]Y. Shapira, S. Finer, and A. Misetish, Phys. Rev. Lett. 23, 98 (1969); Y. Shapira, J. Appl. Phys. 42, 1588 (1971).
[20]E. Domany and M. E. Fisher, Phys. Rev. B 15, 3510 (1977).
[21]K. W. Blazey, H. Rohrer, and R. Webster, Phys. Rev. B 4, 2287 (1971).
[22]H. Rohrer and Ch. Gerber, Phys. Rev. Lett. 38, 909 (1977).
[23]A. R. King and H. Rohrer, AIP Conf. Proc. 29, 476 (1976).
[24]H. Rohrer and H. Thomas, J. Appl. Phys. 40, 1025 (1969).
[25]D. Paquette, V. Jaccarino, and M. Butler, Int. J. Magn. 6, 27 (1974).
[26]Y. H. Wong, F. L. Scarpace, M. Y. Chen, and W. M. Yen, AIP Conf. Proc. 5, 655 (1971).
[27]H. Rohrer (unpublished).
[28]D. R. Nelson, AIP Conf. Proc. 29, 450 (1976); D. R. Nelson and E. Domany, Phys. Rev. B 13, 236 (1976).
[29]I. F. Lynksyntov, V. L. Pokrovskii, and D. E. Khmel'nitskii, Sov. Phys. JETP 42, 923 (1976); A. Aharony, Ann. Israel Phys. Soc. 2, 14 (1978).
[30]K. W. Blazey, K. A. Müller, M. Ondris, and H. Rohrer, Phys. Rev. Lett. 24, 105 (1970); K. W. Blazey, M. Ondris, H. Rohrer, and H. Thomas, J. Phys. (Paris) 32, C1-1020 (1971).
[31]M. E. Fisher, Philos. Mag. 7, 1731 (1962).
[32]D. P. Landau, J. Phys. (Paris) 32, C1-1012 (1971); J. J. White, H. I. Song, J. E. Rives, and D. P. Landau, Phys. Rev. B 4, 4605 (1971).
[33]See, for instance, P. R. Bevington, in *Data Reduction and Error Analysis for the Physical Sciences* (McGraw-Hill, New York, 1969).
[34]A. D. Bruce, J. Phys. C 8, 2992 (1975).
[35]A. R. King and S. M. Rezende (unpublished).